

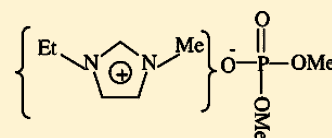
# Measurement and Correlation of Phase Diagram Data for Aqueous Two-Phase Systems Containing 1-Ethyl-3-methylimidazolium Dimethyl Phosphate + $K_3PO_4/K_2HPO_4/K_2CO_3 + H_2O$ Ionic Liquids at (298.15, 308.15, and 318.15) K

Liang Wang,<sup>†</sup> Hong Zhu,<sup>†</sup> Chunhong Ma,<sup>†</sup> Yongsheng Yan,<sup>\*,‡</sup> and Qingwei Wang<sup>\*,†</sup>

<sup>†</sup>College of Chemistry, Jilin Normal University, 1301 Haifeng Road, Siping 136000, People's Republic of China

<sup>‡</sup>School of Chemistry and Chemical Engineering, Jiangsu University, 301 Xuefu Road, Zhenjiang 212013, People's Republic of China

**ABSTRACT:** Binodal data for the 1-ethyl-3-methylimidazolium dimethyl phosphate ([Emim]DMP) + salt ( $K_3PO_4$ ,  $K_2HPO_4$ , and  $K_2CO_3$ ) +  $H_2O$  systems were experimentally determined at  $T = (298.15, 308.15, \text{ and } 318.15) \text{ K}$ , respectively. The Merchuk equation was used to correlate the binodal data. The abilities of the different salts for phase separation follow the order  $K_3PO_4 > K_2HPO_4 > K_2CO_3$ , which may be related to the Gibbs free energy of hydration of the ions ( $\Delta_{\text{hyd}}G$ ). The two-phase area expands with a decrease in temperature, whereas the slope of the tie lines slightly decreases with an increase in temperature. The reliability of the calculation method and corresponding tie-line data was described by the Othmer–Tobias and Bancroft equations, as well as the two-parameter equation. [Emim]DMP is a familiar ionic liquid, extensively used for the extractive desulfurization of fuel oils. This study is the first to report data on the phase diagrams of [Emim]DMP + salt + water systems.



## INTRODUCTION

Liquid–liquid extraction (LLE) is popular, well established, versatile, and easy to use for separation processes.<sup>1</sup> Aqueous two-phase systems (ATPSs), which are usually formed with two incompatible polymers or a polymer and a salt in water above a certain critical concentration, are improved LLE systems.<sup>2–4</sup> Aqueous two-phase extraction (ATPE) is an economical and efficient downstream processing method widely used for the separation, preconcentration, and purification of biomolecules,<sup>5</sup> metallic ions,<sup>6</sup> dye molecules,<sup>7</sup> drug molecules,<sup>8</sup> small organic molecules,<sup>9</sup> and nanoparticles.<sup>10</sup>

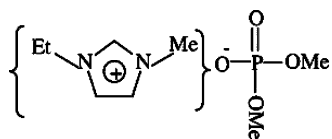


**Figure 1.** Structure of [Emim]DMP.

In recent years, ATPSs based on ionic liquids (ILs) as a new type of LLE have been investigated since Gutowski et al.<sup>11</sup> demonstrated that hydrophilic ILs could form ATPSs when potassium phosphate was added to the aqueous solution. ILs, being typically nonflammable and nonvolatile compounds, may help design environmentally safe processes.<sup>12</sup> Hence, IL-based aqueous two-phase systems (ILATPSs) have been successfully used to separate antibiotics,<sup>13–16</sup> drugs,<sup>17,18</sup> and proteins.<sup>19</sup> These new ATPSs present promising prospects for green extraction and separation processes.<sup>20</sup>

The most common kosmotropic salts employed by different research groups in the IL-based ATPE technique consist of selective cations (ammonium, potassium, or sodium) and

anions (phosphate, sulfate, hydroxide, or carbonate).<sup>21,22</sup> Neves and Ventura<sup>23,24</sup> evaluated cation and anion influence on the formation and extraction capabilities of ILATPSs. The results indicate that the ability of an IL to induce ATPS closely follows the decrease in the hydrogen bond accepting strength or the increase in the hydrogen bond acidity of the IL anion. In the same way, an IL cation also has a significant influence on the behavior of the binodal curves and in the promotion of ATPS. Increasing the alkyl chain length (for mono- or disubstituted ILs) increases the phase separation ability, whereas the insertion of a double bond, a benzyl group, or a hydroxyl group leads to a decrease of ATPS promotion capability. Choosing ILs and salt for ILATPSs is important. Wu and co-workers<sup>25,26</sup> researched the phase diagrams of 1-butyl-3-methylimidazolium tetrafluoroborate ([C<sub>4</sub>mim]BF<sub>4</sub>) + saccharides + water. Pei et al.<sup>27</sup> reported liquid–liquid equilibrium data for imidazolium IL ([C<sub>4</sub>mim]Cl, [C<sub>6</sub>mim]Cl, [C<sub>4</sub>mim]Br, [C<sub>6</sub>mim]Br, [C<sub>8</sub>mim]Br, and [C<sub>10</sub>mim]Br) + salt (KOH,  $K_2HPO_4$ ,  $K_2CO_3$ , and  $K_3PO_4$ ). Deng et al.<sup>28</sup> measured the binodal curves and tie-line data of [Amim]Cl + salt ( $K_3PO_4$ ,  $K_2HPO_4$ , and  $K_2CO_3$ ) + water, which correlated satisfactorily with the Merchuk, Othmer–Tobias, and Bancroft equations, respectively.

1-Ethyl-3-methylimidazolium dimethyl phosphate ([Emim]DMP) is a common and chaotropic IL. The structure of [Emim]DMP is shown in Figure 1. [Emim]DMP was effectively used for the extractive desulfurization of fuel oils.<sup>29,30</sup> It is theoretically composed of ILATPS with conformable kosmotropic salt solutions. The vapor pressure data for water, methanol, ethanol, and their binary mixtures in the presence of [Emim]DMP were measured by

**Received:** November 5, 2010

**Accepted:** January 8, 2012

**Published:** February 3, 2012

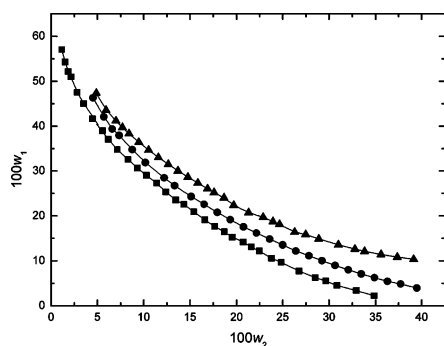


**Figure 2.** Effect of temperature on binodal curves of the [Emim]DMP (1) +  $K_3PO_4$  (2) +  $H_2O$  (3) ATPS: ■, 298.15 K; ●, 308.15 K; ▲, 318.15 K.

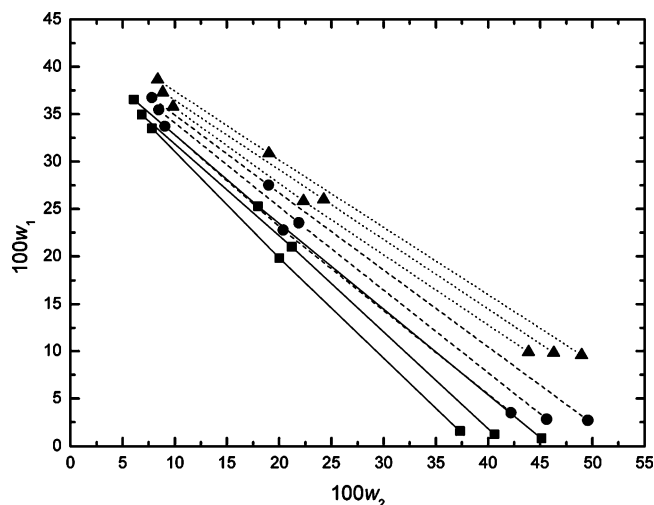


**Figure 3.** Effect of temperature on the equilibrium phase compositions of the [Emim]DMP (1) +  $K_3PO_4$  (2) +  $H_2O$  (3) ATPS: ■, 298.15 K; ●, 308.15 K; ▲, 318.15 K; —, tie lines at 298.15 K; - - -, tie lines at 308.15 K; ···, tie lines at 318.15 K. These tie lines were obtained by connecting the experimental equilibrium phase composition data.

Wang et al.<sup>31</sup> However, data on the phase diagrams of [Emim]DMP + salt + water systems have not been reported.

In the present work, the ILATPS of [Emim]DMP + salt ( $K_3PO_4$ ,  $K_2HPO_4$ , and  $K_2CO_3$ ) +  $H_2O$  was designed. The results show that the ILATPS system is easy to construct. The binodal curves were fitted to the Merchuk equation, and the tie lines were described using the Othmer–Tobias and Bancroft equations, as well as the two-parameter equation. The effects of temperature on the binodal curves and tie lines were also studied. In addition, the ability of the three different salts for phase separation was examined. These results confirm very good correlation and provide a possible basis for the prediction of phase composition when such data are unavailable.

## EXPERIMENTAL SECTION

**Materials.** [Emim]DMP was purchased from Chengjie Chemical Co., Ltd. (Shanghai, China) with a quoted purity greater than 0.99 mass fraction and was used without further purification.  $K_3PO_4$ ,  $K_2CO_3$ , and  $K_2HPO_4$  were analytical-grade reagents (GR, min. 99 % by mass fraction), supplied by Sinopharm Chemical Reagent Co., Ltd. Double-distilled deionized water was used for the experiments.

**Apparatus and Procedures.** The binodal curves were determined by the cloud point method (titration method).

**Table 1.** Binodal Data for the Hydrophilic [Emim]DMP (1) +  $K_3PO_4$  (2) +  $H_2O$  (3) Systems at  $T = (298.15, 308.15, \text{ and } 318.15)$  K and Pressure  $p = 0.1 \text{ MPa}$ <sup>a</sup>

$T = 298.15 \text{ K}$		$T = 308.15 \text{ K}$		$T = 318.15 \text{ K}$	
100 $w_2$	100 $w_1$	100 $w_2$	100 $w_1$	100 $w_2$	100 $w_1$
1.15	57.03	4.52	46.27	4.88	47.34
1.51	54.26	5.70	42.03	5.94	43.56
1.84	52.14	6.60	39.34	7.00	41.14
2.15	50.97	7.35	37.90	7.70	39.68
2.82	47.46	8.76	34.72	8.41	38.31
3.52	44.99	10.17	31.85	9.47	36.41
5.55	38.97	12.21	28.46	10.53	34.66
4.48	41.58	13.35	26.69	11.59	33.02
6.16	37.03	15.12	24.27	12.65	31.48
7.14	34.74	16.53	22.56	13.70	30.02
8.29	32.57	17.94	20.75	14.76	28.63
9.31	30.65	19.35	19.15	15.82	27.30
10.29	29.01	20.77	17.53	16.88	26.03
11.38	27.28	22.18	16.18	17.59	25.21
12.38	25.30	23.59	14.81	18.65	24.01
13.45	23.51	25.01	13.51	19.71	22.36
14.32	22.58	26.42	12.17	21.33	20.70
15.41	20.89	27.83	11.10	22.89	19.68
16.59	19.12	29.24	9.99	23.95	18.72
17.64	17.65	30.66	8.95	24.65	18.10
18.69	16.42	32.07	7.97	26.27	16.37
19.56	15.21	33.48	7.05	27.48	15.84
20.73	14.16	34.89	6.20	28.89	14.85
21.60	13.06	36.31	5.42	31.01	13.53
22.48	12.16	37.72	4.81	32.78	12.59
23.79	10.53	39.48	3.90	33.83	12.10
24.81	9.66			35.60	11.38
26.76	7.72			37.36	10.79
28.50	6.22			39.13	10.32
29.64	5.53				
30.84	4.45				
32.94	3.35				
34.89	2.20				

<sup>a</sup>Standard uncertainties  $u$  are  $u(w) = 0.001$ ,  $u(T) = 0.05 \text{ K}$ , and  $u(p) = 10 \text{ kPa}$ .

From stock, a salt solution of known concentration was placed into a vessel. The pure IL of [Emim]DMP was then added dropwise to the vessel until the mixture became turbid or cloudy. This phenomenon indicates the formation of two liquid phases. Then, water was added dropwise to the vessel to obtain a clear one-phase system, and the above-mentioned procedure was repeated. The vessel was immersed in a jacketed glass vessel, and the system temperature was maintained and controlled within  $\pm 0.05 \text{ K}$  using a DF-101S water thermostat (Gongyi Yuhua Instrument Factory, China). The composition of the mixture for each point on the binodal curve was calculated by mass using an analytical balance (BS 124S, Beijing Sartorius Instrument Co., China) with a precision of  $\pm 0.0001 \text{ g}$ .

For the determination of the tie lines, a series of ATPSs with at least three different known total compositions, mixed with appropriate amounts of [Emim]DMP, salt, and water, were prepared in the vessel. After vigorously stirring for at least 30 min, the system was placed in a thermostatted bath for 12 h. Then, a TDL-4 centrifuge (Shanghai Anke Instrument Factory, China) operated at 2000 rpm was used for 20 min in each test to ensure complete phase separation. The systems were placed

**Table 2. Binodal Data for the Hydrophilic [Emim]DMP (1) + K<sub>2</sub>HPO<sub>4</sub> (2) + H<sub>2</sub>O (3) Systems at T = (298.15, 308.15, and 318.15) K and Pressure p = 0.1 MPa<sup>a</sup>**

T = 298.15 K		T = 308.15 K		T = 318.15 K	
100 w <sub>2</sub>	100 w <sub>1</sub>	100 w <sub>2</sub>	100 w <sub>1</sub>	100 w <sub>2</sub>	100 w <sub>1</sub>
1.76	62.77	2.33	64.21	2.13	69.11
2.75	54.17	3.27	56.53	2.51	66.22
3.79	48.83	4.02	52.80	3.43	59.65
4.70	44.95	5.15	48.35	4.40	56.19
5.64	41.74	6.46	44.81	5.91	50.91
6.56	39.21	7.04	42.79	7.80	45.97
7.59	36.40	8.17	40.13	8.93	43.55
8.61	34.21	9.31	37.80	9.85	42.09
9.54	32.45	10.06	36.40	10.82	40.09
10.58	30.54	11.19	34.47	11.95	38.27
11.64	28.95	12.33	32.70	12.71	37.14
12.68	27.24	13.08	31.60	13.84	35.55
13.46	26.11	14.22	30.05	14.93	34.31
14.90	24.06	15.26	28.12	15.73	33.12
15.41	23.49	17.24	26.34	16.86	31.77
16.68	21.95	19.12	24.29	17.99	30.50
17.57	20.93	20.63	22.75	19.80	28.51
18.56	19.92	22.14	21.11	21.01	27.38
19.71	18.63	24.03	19.63	22.90	25.62
20.29	18.01	25.17	18.67	24.88	23.99
21.92	16.34	26.30	17.77	26.68	22.47
22.73	15.63	27.43	16.89	27.81	21.61
23.60	14.91	28.56	16.06	28.94	20.80
24.97	13.96	29.70	15.27	30.83	19.52
25.90	13.08	31.21	14.28	32.72	18.54
26.99	12.26	32.34	13.79	33.85	17.71
28.15	11.47	34.23	12.49	35.74	16.70
29.33	10.59	35.37	11.89	36.87	16.14
31.67	9.08	36.12	11.51	38.59	15.29
33.41	7.98	37.63	10.79	40.47	15.16
35.04	7.03	38.38	10.45		
37.04	6.08	40.33	10.06		
39.14	5.09				

<sup>a</sup>Standard uncertainties *u* are  $u(w) = 0.001$ ,  $u(T) = 0.05$  K, and  $u(p) = 10$  kPa.

again into the thermostatted bath and allowed to settle for at least 2 h to enable separation into two clear phases. After reaching phase equilibrium, the volumes of the top and bottom phases were noted. The samples of the top and bottom phases were retrieved carefully for analysis. The concentrations of salts in the top and bottom phases were determined by inductively coupled plasma–optical emission spectrometry (VISTA-MPX, US Varian Co., USA). The uncertainty in the measurement of the mass fraction of the salts was estimated to be  $\pm 0.00001$ . The mass fraction of [Emim]DMP in both phases was determined at 210 nm (absorption peak) using a UV–vis spectrometer (model UV-2450, Shimadzu Corporation, Japan). The uncertainty of the mass fraction of [Emim]DMP was better than 0.001. The mass fraction of water was then calculated.

The tie-line length (TLL) and tie-line slope *S* at different compositions were calculated using eqs 1 and 2, respectively.

$$\text{TLL} = [(w_1^t - w_1^b)^2 + (w_2^t - w_2^b)^2]^{0.5} \quad (1)$$

$$S = (w_1^t - w_1^b)/(w_2^t - w_2^b) \quad (2)$$

**Table 3. Binodal Data for the Hydrophilic [Emim]DMP (1) + K<sub>2</sub>CO<sub>3</sub> (2) + H<sub>2</sub>O (3) Systems at T = (298.15, 308.15, and 318.15) K and Pressure p = 0.1 MPa<sup>a</sup>**

T = 298.15 K		T = 308.15 K		T = 318.15 K	
100 w <sub>2</sub>	100 w <sub>1</sub>	100 w <sub>2</sub>	100 w <sub>1</sub>	100 w <sub>2</sub>	100 w <sub>1</sub>
1.20	77.12	2.98	80.16	2.61	94.96
1.53	73.21	3.72	74.43	3.56	85.43
1.86	70.36	4.84	67.01	4.37	80.22
2.24	68.29	5.95	61.12	5.11	75.06
2.61	65.97	6.69	57.8	6.03	70.08
3.01	63.18	7.80	54.27	7.26	64.43
3.51	60.95	8.64	51.83	8.96	58.50
4.32	56.74	9.66	48.88	10.01	55.34
5.07	54.07	10.77	45.81	11.63	51.20
5.68	51.57	11.80	42.97	14.19	46.34
6.81	48.09	12.92	40.73	16.28	42.70
7.79	45.29	13.73	39.51	18.39	39.63
8.81	42.94	14.85	37.80	20.37	36.81
9.81	40.58	15.96	35.80	22.24	34.59
10.62	38.98	17.11	33.62	24.38	32.08
11.83	36.76	18.92	31.37	27.13	30.07
13.04	34.70	20.78	28.80	29.51	28.08
13.86	33.23	21.89	27.65	31.79	26.56
14.99	31.69	23.43	25.63	33.74	25.75
16.28	29.81	24.55	24.90	35.66	24.54
16.94	28.49	25.97	23.62	37.01	23.89
17.60	27.46	27.82	21.16	39.31	22.66
18.07	26.70	28.93	20.36		
19.36	25.10	30.86	18.54		
20.49	23.38	32.64	17.09		
21.51	22.23	34.64	15.75		
22.16	21.38	35.98	15.02		
23.74	19.24	37.83	14.05		
24.72	18.34	38.94	13.81		
25.60	17.18				
27.05	15.28				
28.11	14.40				
29.37	12.99				
30.88	11.53				
33.10	9.68				
35.97	7.20				
38.06	5.95				

<sup>a</sup>Standard uncertainties *u* are  $u(w) = 0.001$ ,  $u(T) = 0.05$  K, and  $u(p) = 10$  kPa.

where  $w_1^t$ ,  $w_1^b$ ,  $w_2^t$ , and  $w_2^b$  represent the equilibrium mass fraction of [Emim]DMP (1) and salt (2) in the top (t) and bottom (b) phases, respectively.

## RESULTS AND DISCUSSION

**Binodal Data and Correlation.** For the [Emim]DMP (1) + salt (K<sub>3</sub>PO<sub>4</sub>, K<sub>2</sub>HPO<sub>4</sub>, and K<sub>2</sub>CO<sub>3</sub>) (2) + H<sub>2</sub>O (3) systems, the binodal data determined at T = (298.15, 308.15, and 318.15) K are given in Tables 1, 2, and 3, respectively. The binodal data were correlated using the Merchuk equation

$$w_1 = a \exp(bw_2^{0.5} - cw_2^3) \quad (3)$$

where  $w_1$  is the mass fraction of hydrophilic ILs [Emim]DMP,  $w_2$  is the mass fraction of salts, and *a*, *b*, and *c* represent the fitting parameters. The parameters for this equation were determined by least-squares regression of the cloud point data.

**Table 4.** Values of Parameters of Eq 3 for the Hydrophilic [Emim]DMP (1) + K<sub>3</sub>PO<sub>4</sub>/K<sub>2</sub>HPO<sub>4</sub>/K<sub>2</sub>CO<sub>3</sub> (2) + H<sub>2</sub>O (3) Systems at  $T = (298.15, 308.15, \text{ and } 318.15) \text{ K}^a$ 

$T/\text{K}$	$a$	$b$	$c$	$R^2$	100 SD
[Emim]DMP + K <sub>3</sub> PO <sub>4</sub> + H <sub>2</sub> O					
298.15	78.5560	-0.2984	$4.0932 \times 10^{-5}$	0.9999	0.1668
308.15	93.1704	-0.3304	$1.7820 \times 10^{-5}$	0.9999	3.6412
318.15	93.3979	-0.3064	$6.6189 \times 10^{-6}$	0.9981	1.4872
[Emim]DMP + K <sub>2</sub> HPO <sub>4</sub> + H <sub>2</sub> O					
298.15	98.8349	-0.3573	$1.1736 \times 10^{-5}$	0.9995	0.3045
308.15	103.1037	-0.3268	$4.5731 \times 10^{-6}$	0.9992	1.5548
318.15	103.6012	-0.2875	$2.0711 \times 10^{-6}$	0.9993	3.3271
[Emim]DMP + K <sub>2</sub> CO <sub>3</sub> + H <sub>2</sub> O					
298.15	106.4949	-0.3000	$1.8473 \times 10^{-5}$	0.9999	0.2443
308.15	145.3200	-0.3500	$3.3300 \times 10^{-6}$	0.9995	0.9795
318.15	160.9302	-0.3349	$-2.6946 \times 10^{-6}$	0.9993	18.1146

<sup>a</sup>SD =  $(\sum_{i=1}^n (w_1^{\text{cal}} - w_1^{\text{exp}})^2 / N)^{0.5}$ , where  $w_1$  and  $N$  represent the mass fraction of [Emim]DMP and the number of binodal data, respectively.  $w_1^{\text{exp}}$  is the experimental mass fraction of [Emim]DMP listed in Table 1, and  $w_1^{\text{cal}}$  is the corresponding data calculated using eq 3.

**Table 5.** Tie Line Data of [Emim]DMP (1) + K<sub>3</sub>PO<sub>4</sub> (2) + H<sub>2</sub>O (3) at  $T = (298.15, 308.15, \text{ and } 318.15) \text{ K}$  and Pressure  $p = 0.1 \text{ MPa}^a$ 

$T/\text{K}$	total system		IL-rich phase		salt-rich phase		TLL	S
	100 $w_2$	100 $w_1$	100 $w_2$	100 $w_1$	100 $w_2$	100 $w_1$		
298.15	21.20	21.00	6.82	34.95	40.61	1.23	47.73	-1.00
	20.03	19.82	7.81	33.50	37.33	1.57	43.49	-1.08
	17.99	25.28	6.08	36.54	45.13	0.80	52.93	-0.92
308.15	21.88	23.53	8.48	35.43	45.61	2.83	49.41	-0.88
	20.39	22.78	9.05	33.72	42.22	3.52	44.86	-0.91
	18.99	27.52	7.81	36.74	49.57	2.70	53.88	-0.82
318.15	24.27	26.21	8.85	37.31	46.30	9.82	46.46	-0.73
	22.33	25.83	9.83	35.81	43.86	9.91	42.77	-0.76
	19.01	30.86	8.35	38.64	48.97	9.60	49.93	-0.72

<sup>a</sup>Standard uncertainties  $u$  are  $u(w) = 0.001$ ,  $u(T) = 0.05 \text{ K}$ , and  $u(p) = 10 \text{ kPa}$ .

**Table 6.** Tie Line Data of [Emim]DMP (1) + K<sub>2</sub>HPO<sub>4</sub> (2) + H<sub>2</sub>O (3) at  $T = (298.15, 308.15, \text{ and } 318.15) \text{ K}$  and Pressure  $p = 0.1 \text{ MPa}^a$ 

$T/\text{K}$	total system		IL-rich phase		salt-rich phase		TLL	S
	100 $w_2$	100 $w_1$	100 $w_2$	100 $w_1$	100 $w_2$	100 $w_1$		
298.15	25.96	26.98	4.22	44.87	57.04	0.43	69.02	-0.84
	22.01	26.43	6.00	39.99	49.66	2.22	57.73	-0.87
	19.99	30.50	5.11	42.57	53.88	1.24	63.93	-0.85
308.15	24.57	34.03	4.42	50.87	56.04	8.03	67.07	-0.83
	20.08	33.33	5.80	46.00	50.66	8.62	58.40	-0.83
	23.09	28.00	7.61	41.00	45.88	9.31	49.68	-0.83
318.15	26.57	36.82	4.82	54.69	56.04	12.93	66.08	-0.82
	21.21	36.33	6.64	49.00	50.16	13.62	56.09	-0.81
	20.10	43.90	4.02	57.32	58.58	13.26	70.13	-0.81

<sup>a</sup>Standard uncertainties  $u$  are  $u(w) = 0.001$ ,  $u(T) = 0.05 \text{ K}$ , and  $u(p) = 10 \text{ kPa}$ .

Recently, the above equation has been successfully used for the correlation of binodal data of IL + salt<sup>21,22,25,27</sup> ATPSs. Using eq 3, the coefficients  $a$ ,  $b$ , and  $c$  obtained from the correlation of experimental binodal data along with the correlation coefficients ( $R$ ) and standard deviations (SD) are given in Tables 4. On the basis of obtained standard deviations, we concluded that eq 3 can be satisfactorily used to correlate the binodal curves of the investigated systems.

**Effect of Temperature on Binodal Curves.** The effects of temperature on the phase-forming ability of the studied system are illustrated in Figure 2. The loci of the experimental

binodals demonstrate that the two-phase area expands with a decrease in temperature for [Emim]DMP + K<sub>3</sub>PO<sub>4</sub> + H<sub>2</sub>O. This phenomenon is attributed to the decrease in the solubility of IL or the increase in the phase-forming ability of salt in the studied system. More recently, the effect of temperature on the phase-forming ability in the [Bmim]BF<sub>4</sub> + (NH<sub>4</sub>)<sub>2</sub>SO<sub>4</sub> two-phase system<sup>32</sup> has also demonstrated that the two-phase area expands with a decrease in temperature.

**Effect of Salts on Binodal Curves.** The phase diagrams in Figure 2 also provide information on the concentration of phase-forming components required to form two phases and

**Table 7. Tie Line Data of [Emim]DMP (1) + K<sub>2</sub>CO<sub>3</sub> (2) + H<sub>2</sub>O (3) at  $T = (298.15, 308.15, \text{ and } 318.15)$  K and Pressure  $p = 0.1$  MPa<sup>a</sup>**

T/K	total system		IL-rich phase		salt-rich phase		TLL	S
	100 $w_2$	100 $w_1$	100 $w_2$	100 $w_1$	100 $w_2$	100 $w_1$		
298.15	19.98	35.18	4.98	53.35	48.57	3.45	66.26	-1.14
	18.07	41.06	3.88	57.48	52.35	2.92	72.98	-1.13
	22.02	40.16	2.77	62.45	55.74	2.33	80.13	-1.14
308.15	21.84	39.28	7.08	56.05	47.72	12.05	59.89	-1.08
	19.17	45.16	6.19	59.48	51.60	11.52	66.04	-1.06
	22.92	45.96	5.47	63.85	56.54	11.03	73.48	-1.03
318.15	21.69	50.88	6.48	67.15	52.87	20.55	65.75	-1.00
	19.57	57.86	5.59	72.38	57.10	20.02	73.45	-1.02
	24.02	56.66	4.67	77.35	61.54	19.53	81.11	-1.02

<sup>a</sup>Standard uncertainties  $u$  are  $u(w) = 0.001$ ,  $u(T) = 0.05$  K, and  $u(p) = 10$  kPa.

**Table 8. Values of the Parameters of Eqs 4 and 5 for the [Emim]DMP (1) + K<sub>3</sub>PO<sub>4</sub>/K<sub>2</sub>HPO<sub>4</sub>/K<sub>2</sub>CO<sub>3</sub> (2) + H<sub>2</sub>O (3) ATPS at  $T = (298.15, 308.15 \text{ and } 318.15)$  K<sup>a</sup>**

T/K	Othmer–Tobias equation				Bancroft equation			
	$k_1$	$n$	$R$	$\delta$	$k_2$	$r$	$R$	$\delta$
[Emim]DMP + K <sub>3</sub> PO <sub>4</sub> + H <sub>2</sub> O								
298.15	1.5994	0.4112	0.9923	0.0015	0.3298	2.8650	0.9976	0.0019
308.15	1.7011	0.4441	0.9700	0.0029	0.3619	2.4183	0.9423	0.0087
318.15	1.5462	0.5905	0.9918	0.0014	0.4275	2.1646	0.9992	0.0008
[Emim]DMP + K <sub>2</sub> HPO <sub>4</sub> + H <sub>2</sub> O								
298.15	1.4899	0.6708	0.9966	0.0015	0.6144	1.5069	0.9967	0.0019
308.15	1.2177	0.9760	0.9955	0.0033	0.7517	1.1849	0.9953	0.0036
318.15	1.0482	0.9812	0.9996	0.0009	0.8299	1.3724	0.9975	0.0026
[Emim]DMP + K <sub>2</sub> CO <sub>3</sub> + H <sub>2</sub> O								
298.15	0.8195	1.2988	0.9835	0.0060	1.1928	0.7993	0.9788	0.0050
308.15	0.7215	0.9200	0.9999	0.0004	1.4049	1.2237	0.9996	0.0010
318.15	0.5774	1.4462	0.9999	0.0003	1.2110	0.9363	0.9985	0.0024

<sup>a</sup> $R$ , corresponding correlation coefficient values;  $\delta$ , standard deviation.

**Table 9. Values of Parameters of Eq 6 for the [Emim]DMP (1) + K<sub>3</sub>PO<sub>4</sub>/K<sub>2</sub>HPO<sub>4</sub>/K<sub>2</sub>CO<sub>3</sub> (2) + H<sub>2</sub>O (3) ATPS at  $T = (298.15, 308.15 \text{ and } 318.15)$  K<sup>a</sup>**

T/K	$k$	$\beta$	$R$	$\delta$
[Emim]DMP + K <sub>3</sub> PO <sub>4</sub> + H <sub>2</sub> O				
298.15	0.1158	2.1294	0.9977	0.0061
308.15	0.0782	0.8349	0.9313	0.0234
318.15	0.0871	0.7541	0.9845	0.0099
[Emim]DMP + K <sub>2</sub> HPO <sub>4</sub> + H <sub>2</sub> O				
298.15	0.0733	0.6624	0.9960	0.0089
308.15	0.0665	0.3145	0.9996	0.0043
318.15	0.0740	0.6044	0.9842	0.0242
[Emim]DMP + K <sub>2</sub> CO <sub>3</sub> + H <sub>2</sub> O				
298.15	0.0709	1.2645	0.9999	0.0022
308.15	0.0483	0.2116	0.9934	0.0100
318.15	0.0427	-0.1009	0.9951	0.0097

<sup>a</sup> $R$ , corresponding correlation coefficient values;  $\delta$ , standard deviation.

the concentration of phase components in the top and bottom phases. The diagrams show that ILATPS can be formed by mixing an appropriate amount of salts with aqueous [Emim]DMP solution. Thus, the abilities of the salts for phase separation follow the order K<sub>3</sub>PO<sub>4</sub> > K<sub>2</sub>HPO<sub>4</sub> > K<sub>2</sub>CO<sub>3</sub>. The kosmotropic ions, PO<sub>4</sub><sup>3-</sup>, HPO<sub>4</sub><sup>2-</sup>, and CO<sub>3</sub><sup>2-</sup>, which exhibit stronger interaction with water molecules, are beneficial to ILATPS formation. The salting-out ability may be related to the Gibbs energy of hydration of the ions ( $\Delta_{\text{hyd}}G$ ).<sup>33,34</sup> Considering that these salts share a

common cation but contain different anions, better salting-out of [Emim]DMP was observed when the ions of the salt have a more negative Gibbs free energy { $\Delta_{\text{hyd}}G(\text{PO}_4^{3-}) = -2765 \text{ kJ}\cdot\text{mol}^{-1}$ ,  $26 > \Delta_{\text{hyd}}G(\text{HPO}_4^{2-}) = -1789 \text{ kJ}\cdot\text{mol}^{-1}$ ,  $27 > \Delta_{\text{hyd}}G(\text{CO}_3^{2-}) = -1315 \text{ kJ}\cdot\text{mol}^{-1}$ }.<sup>35,36</sup>

**LLE Data and Effect of Temperature on Tie Lines.** The tie-line compositions, TLL, and  $S$  for the [Emim]DMP + salt (K<sub>3</sub>PO<sub>4</sub>, K<sub>2</sub>HPO<sub>4</sub>, and K<sub>2</sub>CO<sub>3</sub>) + H<sub>2</sub>O systems determined at  $T = (298.15, 308.15, \text{ and } 318.15)$  K are given in Tables 5, 6, and 7, respectively. Additionally, to show the effect of temperature on the equilibrium phase compositions in the investigated system, the experimental tie lines are compared in Figure 3 for the temperatures  $T = (298.15, 308.15, \text{ and } 323.15)$  K. Figure 3 shows that the slope of the tie lines slightly decreases with an increase in temperature. This trend indicates that when temperature decreases, water is driven from the [Emim]DMP-rich phase to the salt-rich phase, so that the [Emim]DMP concentration at the [Emim]DMP-rich phase increases. Conversely, that at the salt-rich phase is somewhat more diluted. In other words, water becomes a poorer solvent for [Emim]DMP as temperature decreases.

**Correlation of LLE Data.** The Othmer–Tobias (eq 4) and Bancroft (eq 5) equations were used to evaluate the reliability of the calculation method and corresponding tie-line data.

$$[(1 - w_1^t)/w_1^t] = k_1[(1 - w_2^b)/w_2^b]^n \quad (4)$$

$$(w_3^b/w_2^b) = k_2(w_3^t/w_1^t)^r \quad (5)$$

where  $w_1^t$  is the mass fraction of ILs in the top phase;  $w_2^b$  denotes the mass fraction of salt in the bottom phase;  $w_3^b$  and  $w_3^t$  are the mass fractions of water in the bottom and top phases, respectively; and  $k_1$ ,  $n$ ,  $k_2$ , and  $r$  represent the fit parameters. Recently, eqs 4 and 5 have been successfully used for the correlation of the tie-line compositions of the imidazolium ILs + salt + water ATPSS.<sup>37,38</sup> A linear dependency of the plot  $\log[(1 - w_1^t)/w_1^t]$  against  $\log[(1 - w_2^b)/w_2^b]$  and  $\log(w_3^b/w_2^b)$  against  $\log(w_3^t/w_1^t)$ , indicates acceptable consistency of the results. The values of  $k_1$ ,  $n$ ,  $k_2$ , and  $r$  with the corresponding correlation coefficient values ( $R$ ) and SDs ( $\delta$ ) are given in Table 8. Equations 4 and 5 can be satisfactorily used to correlate the tie-line data of the investigated systems.

In this work, a relatively simple two-parameter equation was used to correlate the tie-line data, which can be derived from the binodal theory.<sup>39</sup> The equation used has the following form:

$$\ln(w_2^t/w_2^b) = \beta + k(w_1^b - w_1^t) \quad (6)$$

where  $k$  is the salting-out coefficient and  $\beta$  is the constant related to the activity coefficient. Superscripts t and b denote the IL-rich and salt-rich phases, respectively. Recently, eq 6 has been successfully used for the correlation of tie-line data for the polymer-salt ATPSS.<sup>40</sup> The fitting parameters of eq 6 with the corresponding correlation coefficient values ( $R$ ) and SDs ( $\delta$ ) for the investigated systems are presented in Table 9. On the basis of the SDs reported, eq 6 reveals good accuracy for the experimental LLE data.

## CONCLUSIONS

The binodal data of the [Emim]DMP + salt ( $K_3PO_4$ ,  $K_2HPO_4$ , and  $K_2CO_3$ ) +  $H_2O$  systems were determined at  $T = (298.15, 308.15, \text{ and } 318.15) \text{ K}$ , respectively. The experimental binodal data directly calculated using the Merchuk equation exhibits optimum accuracy. The abilities of the kosmotropic salts for phase separation follow the order  $K_3PO_4 > K_2HPO_4 > K_2CO_3$ , which can be explained by the Gibbs free energy of hydration of anions. The two-phase area expands with a decrease in temperature, whereas the slope of the tie lines slightly decreases with an increase in temperature. Finally, the tie lines were correlated with the Othmer–Tobias and Bancroft equations, as well as with the two-parameter equation, which show satisfactory accuracy for the investigated systems.

## AUTHOR INFORMATION

### Corresponding Author

\*Tel: +086051188790683. Fax: +086051188791800. E-mail: yys@ujes.edu.cn or zh123002@sina.com (Y.Y.); wqw611223@163.com (Q.W.).

### Funding

This work was financially supported by the National Natural Science Foundation (Grant No. 21076098), the Jilin Province Education Foundation (Grant No. 2009195), and Jiangsu University Ph.D. Innovative Projects (Grant No. CX09B\_199Z).

## REFERENCES

- Lo, T. C. In *Handbook of Separation Techniques for Chemical Engineers*; Schwietzer, P. A., Ed.; McGraw-Hill: New York, 1996.
- Albertsson, P. Å. *Partition of Cell Particles and Macromolecules: Separation and Purification of Biomolecules, Cell Organelles, Membranes, and Cells in Aqueous Polymer Two-Phase Systems and Their Use in*

*Biochemical Analysis and Biotechnology*, 3rd ed.; Wiley: New York, 1986; p 22.

(3) Walter, H.; Brooks, D. E.; Fisher, D. *Partitioning in Aqueous Two-Phase Systems: Theory, Methods, Uses, and Applications to Biotechnology*; Academic Press: New York, 1985.

(4) Zaslavsky, B. Y. *Aqueous Two-Phase Partitioning: Physical Chemistry and Bioanalytical Applications*; Marcel Dekker: New York, 1995.

(5) Johansson, H. O.; Magaldi, F. M.; Feitosa, E.; Pessoa, A. Jr. Protein partitioning in poly(ethylene glycol)/sodium polyacrylate aqueous two-phase systems. *J. Chromatogr., A* **2008**, *1178*, 145–153.

(6) Bulgariu, L.; Bulgariu, D. Extraction of metal ions in aqueous polyethylene glycol-inorganic salt two-phase systems in the presence of inorganic extractants: Correlation between extraction behaviour and stability constants of extracted species. *J. Chromatogr., A* **2008**, *1196–1197*, 117–124.

(7) Mageste, A. B.; de Lemos, L. R.; Ferreira, G. M. D. Aqueous two-phase systems: An efficient, environmentally safe and economically viable method for purification of natural dye carmine. *J. Chromatogr., A* **2009**, *1216* (45), 7623–7629.

(8) Agasoster, T. Aqueous two-phase partitioning sample preparation prior to liquid chromatography of hydrophilic drugs in blood. *J. Chromatogr., B* **1998**, *716*, 293–298.

(9) Willauer, H. D.; Huddleston, J. G.; Rogers, R. D. Solute partitioning in aqueous biphasic systems composed of polyethylene glycol and salt: The partitioning of small neutral organic species. *Ind. Eng. Chem. Res.* **2002**, *41* (7), 1892–1904.

(10) Negrete, A.; Ling, T. C.; Lyddiatt, A. Aqueous two-phase recovery of bio-nanoparticles: A miniaturization study for the recovery of bacteriophage T4. *J. Chromatogr., B* **2007**, *854* (1–2), 13–19.

(11) Gutowski, K. E.; Broker, G. A.; Willauer, H. D.; Huddleston, J. G.; Swatoski, R. P.; Holbrey, J. D.; Rogers, R. D. Controlling the aqueous miscibility of ionic liquids: Aqueous biphasic systems of water-miscible ionic liquids and water-structuring salts for recycle, metathesis, and separations. *J. Am. Chem. Soc.* **2003**, *125*, 6632–6633.

(12) Mihkel, K. *Ionic Liquids in Chemical Analysis*; CRC Press: New York, 2009; p 244.

(13) Soto, A.; Arce, A.; Khoshkbarchi, M. K. Partitioning of antibiotics in a two-liquid phase system formed by water and a room temperature ionic liquid. *Sep. Purif. Technol.* **2005**, *44*, 242–246.

(14) Jiang, Y.; Xia, H.; Guo, C.; Mahmood, I.; Liu, H. Phenomena and mechanism for separation and recovery of penicillin in ionic liquids aqueous solution. *Ind. Eng. Chem. Res.* **2007**, *46*, 6303–6312.

(15) Li, C. X.; Han, J.; Wang, Y.; Yan, Y. S.; Xu, X. H.; Pan, J. M. Extraction and mechanism investigation of trace roxithromycin in real water samples by use of ionic liquid-salt aqueous two-phase system. *Anal. Chim. Acta* **2009**, *653*, 178–183.

(16) Liu, Q. F.; Yu, J.; Li, W. L.; Hu, X. S.; Xia, H. S.; Liu, H. Z.; Yang, P. Partitioning behavior of penicillin g in aqueous two phase system formed by ionic liquids and phosphate. *Sep. Sci. Technol.* **2006**, *41*, 2849–2858.

(17) He, C.; Li, S.; Liu, H.; Li, K.; Liu, F. Extraction of testosterone and epitestosterone in human urine using aqueous two-phase systems of ionic liquid and salt. *J. Chromatogr., A* **2005**, *1082*, 143–149.

(18) Li, S.; He, C.; Liu, H.; Li, K.; Liu, F. Ionic liquid-based aqueous two-phase system, a sample pretreatment procedure prior to high-performance liquid chromatography of opium alkaloids. *J. Chromatogr., B* **2005**, *826*, 58–62.

(19) Du, Z.; Yu, Y. L.; Wang, J. H. Extraction of proteins from biological fluids by use of an ionic liquid/aqueous two-phase system. *Chem.—Eur. J.* **2007**, *13*, 2130–2137.

(20) Li, Z. Y.; Pei, Y. C.; Wang, H. Y.; Fan, J.; Wang, J. J. Ionic liquid-based aqueous two-phase systems and their applications in green separation processes. *Trends Anal. Chem.* **2010**, *29* (11), 1336–1346.

(21) Zafarani-Moattar, M. T.; Hamzehzadeh, S. Phase diagrams for the aqueous two-phase ternary system containing the ionic liquid 1-butyl-3-methylimidazolium bromide and tri-potassium citrate at  $T = (278.15, 298.15, \text{ and } 318.15) \text{ K}$ . *J. Chem. Eng. Data* **2009**, *54*, 833–841.

- (22) Han, J.; Pan, R.; Xie, X. Q.; Wang, Y.; Yan, Y. S.; Yin, G. W.; Guan, W. X. Liquid-liquid equilibria of ionic liquid 1-butyl-3-methylimidazolium tetrafluoroborate + sodium and ammonium citrate aqueous two-phase systems at (298.15, 308.15, and 323.15) K. *J. Chem. Eng. Data* **2010**, *55*, 3749–3754.
- (23) Neves, C. M. S. S.; Ventura, S. P. M.; Freire, M. G.; Marrucho, I. M.; Coutinho, J. A. P. Evaluation of cation influence on the formation and extraction capability of ionic-liquid-based aqueous biphasic systems. *J. Phys. Chem. B* **2009**, *113*, 5194–5199.
- (24) Ventura, S. P. M.; Neves, C. M. S. S.; Freire, M. G.; Marrucho, I. M.; Oliveira, J.; Coutinho, J. A. P. Evaluation of anion influence on the formation and extraction capacity of ionic-liquid-based aqueous biphasic systems. *J. Phys. Chem. B* **2009**, *113*, 9304–9310.
- (25) Wu, B.; Zhang, Y. M.; Wang, H. P. Aqueous biphasic systems of hydrophilic ionic liquids + sucrose for separation. *J. Chem. Eng. Data* **2008**, *53*, 983–985.
- (26) Wu, B.; Zhang, Y. M.; Wang, H. P. Phase behavior for ternary systems composed of ionic liquid + saccharides + water. *J. Phys. Chem. B* **2008**, *112*, 6426–6429.
- (27) Pei, Y.; Wang, J.; Liu, L.; Wu, K.; Zhao, Y. Liquid-liquid equilibria of aqueous biphasic systems containing selected imidazolium ionic liquids and salts. *J. Chem. Eng. Data* **2007**, *52*, 2026–2031.
- (28) Deng, Y. F.; Long, T.; Zhang, D. L.; Chen, J.; Gan, S. C. Phase diagram of [Amim]Cl + salt aqueous biphasic systems and its application for [Amim]Cl recovery. *J. Chem. Eng. Data* **2009**, *54* (9), 2470–2473.
- (29) Jiang, X. C.; Nie, Y.; Li, C. X.; Wang, Z. H. Imidazolium-based alkylphosphate ionic liquids: A potential solvent for extractive desulfurization of fuel. *Fuel* **2008**, *87*, 79–84.
- (30) Nie, Y.; Li, C. X.; Meng, H.; Wang, Z. H. N-Dialkylimidazolium dialkylphosphate ionic liquids: Their extractive performance for thiophene series compounds from fuel oils versus the length of alkyl group. *Fuel Process. Technol.* **2008**, *89*, 978–983.
- (31) Wang, J. F.; Li, C. X.; Wang, Z. H.; Li, Z. J.; Jiang, Y. B. Vapor pressure measurement for water, methanol, ethanol, and their binary mixtures in the presence of an ionic liquid 1-ethyl-3-methylimidazolium dimethylphosphate. *Fluid Phase Equilib.* **2007**, *255*, 186–192.
- (32) Wang, Y.; Xu, X. H.; Yan, Y. S.; Han, J.; Zhang, Z. L. Phase behavior for the [Bmim]BF<sub>4</sub> aqueous two-phase systems containing ammonium sulfate/sodium carbonate salts at different temperatures: Experimental and correlation. *Thermochim. Acta* **2010**, *501*, 112–118.
- (33) Zafarani-Moattar, M. T.; Hamzehzadeh, S. Liquid-liquid equilibria of aqueous two-phase systems containing polyethylene glycol and sodium succinate or sodium formate. *CALPHAD: Comput. Coupling Phase Diagrams Thermochem.* **2005**, *29*, 1–6.
- (34) Rogers, R. D.; Bond, A. H.; Bauer, C. B.; et al. Metal ion separations in polyethylene glycol-based aqueous biphasic systems: correlation of partitioning behavior with available thermodynamic hydration data. *J. Chromatogr., B* **1996**, *680*, 221–229.
- (35) Marcus, Y. Thermodynamics of solvation of ions part 5.4 Gibbs free energy of hydration at 298.15 K. *J. Chem. Soc., Faraday Trans.* **1991**, *87* (18), 2995–2999.
- (36) Zafarani-Moattar, M. T.; Zaferanloo, A. Measurement and correlation of phase equilibria in aqueous two-phase systems containing polyvinylpyrrolidone and di-potassium tartrate or di-potassium oxalate at different temperatures. *J. Chem. Thermodyn.* **2009**, *41*, 864–871.
- (37) Li, C. X.; Han, J.; Wang, Y.; Yan, Y. S.; Pan, J. M.; Xu, X. H.; Zhang, Z. L. Phase behavior for the aqueous two-phase systems containing the ionic liquid 1-butyl-3-methylimidazolium tetrafluoroborate and kosmotropic salts. *J. Chem. Eng. Data* **2010**, *55*, 1087–1092.
- (38) Han, J.; Yu, C. L.; Wang, Y.; Xie, X. Q.; Yan, Y. S.; Yin, G. W.; Guan, W. X. Liquid-liquid equilibria of ionic liquid 1-butyl-3-methylimidazolium tetrafluoroborate and sodium citrate/tartrate/acetate aqueous two-phase systems at 298.15 K: Experiment and correlation. *Fluid Phase Equilib.* **2010**, *295*, 98–103.
- (39) Guan, Y.; Lilley, T. H.; Treffry, T. E. A new excluded volume theory and its application to the coexistence curves of aqueous polymer two-phase systems. *Macromolecules* **1993**, *26*, 3971–3979.
- (40) Zafarani-Moattar, M. T.; Seifi-Aghjekohal, P. Liquid-liquid equilibria of aqueous two-phase systems containing polyvinylpyrrolidone and tripotassium phosphate or dipotassium hydrogen phosphate: experiment and correlation. *CALPHAD: Comput. Coupling Phase Diagrams Thermochem.* **2007**, *31*, 553–559.